https://doi.org/10.5194/egusphere-2024-1456
Preprint. Discussion started: 5 June 2024

Evaluating downscaled products with expected hydroclimatic co-variances

Authors: Seung H. Baek[1*], Paul A. Ullrich[1], Bo Dong[1], Jiwoo Lee[1]

Affiliations:

[1]Atmospheric, Earth, & Energy Division, Lawrence Livermore National Laboratory, Livermore, California USA

*Corresponding author. Email: baek1@llnl.gov

Abstract: There has been widespread adoption of downscaled products amongst practitioners and stakeholders to ascertain risk from climate hazards at the local scale. Such products must nevertheless be consistent with physical laws to be credible and of value to users. Here we evaluate statistically and dynamically downscaled products by examining locally relevant covariances between downscaled temperature and precipitation during convective and frontal precipitation events. We find that two widely-used statistical downscaling techniques (LOCalized Analogs version 2 (LOCA2) and Seasonal Trends and Analysis of Residuals Empirical-Statistical Downscaling Model (STAR-ESDM)) generally preserve expected covariances during convective precipitation events over the historical and future projected intervals. However, both techniques dampen future intensification of frontal precipitation that is otherwise robustly captured in global climate models (*i.e.,* prior to downscaling) and with dynamical downscaling. In the case of LOCA2, this leads to appreciable underestimation of future frontal precipitation events. More broadly, our results suggest that statistical downscaling techniques may be limited in their ability to resolve non-stationary hydrologic processes as compared to dynamical downscaling. Finally, our work proposes expected covariances during convective and frontal precipitation as useful evaluation diagnoses that can be applied universally to a wide range of statistically downscaled products.

https://doi.org/10.5194/egusphere-2024-1456
Preprint. Discussion started: 5 June 2024

1. Introduction:

Extreme weather events are among the costliest disasters to the United States. Over the past four decades (1980-2023), there have been more than 370 billion-dollar disasters that cumulatively cost over 2.6 trillion dollars (NOAA, 2023). To ascertain risk from climate hazards, a broad community of practitioners, stakeholders and policymakers rely on historical reconstructions and future projections of local to regional climate that are "downscaled" from coarse global climate model outputs (Fiedler et al. 2021, Pitman et al. 2022). This is because global climate model (GCM) data alone are too coarse in resolution: GCM outputs from the Coupled Model Intercomparison Project 6 (CMIP6), for instance, have grid spacing of ~100 to 300 kilometers in the midlatitudes and cannot adequately represent finer scale features like topography and extreme storms (Eyring et al. 2016).

Numerous climate data products have emerged over the last several years that represent the contiguous United States at local scales, including dynamically and statistically downscaled products. Dynamically downscaled products (*e.g.,* Jones et al. 2022; Liu et al. 2017; Dai et al. 2020; Rasmussen et al. 2023; Chen et al. 2023) use regional climate models that simulate local meteorology, providing a comprehensive set of climate variables that are inherently self-consistent. Because they are generated by a modeling system based on physical laws, dynamical downscaling implicitly preserves physical relationships among variables, although there are biases that arise from insufficient representation of relevant physical processes (such as eddies or extremes; Lee and Hong 2014; Xu et al. 2019) that must be considered. Statistically downscaled products (*e.g.,* Abatzoglou and Brown, 2012; Thrasher et al. 2012, 2022; Pierce et al. 2014, 2023) are derived based on relationships between coarse climate model outputs and observed local meteorology. Since they are generated through simple functional relationships, statistically downscaled products can be generated more rapidly than dynamically downscaled products

https://doi.org/10.5194/egusphere-2024-1456
Preprint. Discussion started: 5 June 2024

(albeit for fewer variables, as dense observational networks are only available for select quantities).

Given their computational convenience, there has been widespread adoption of statistically downscaled products. Statistically downscaled products must nevertheless be both salient and credible to be of value to users; the data must not only be relevant for informing decision-making, but to be trusted for future projections must also be consistent with physical laws (Cash et al., 2002). Importantly, common statistical downscaling methods do not explicitly account for covariances across variables at the local scale (notwithstanding existing covariances generated by climate models prior to downscaling). This may be problematic, as the loss of process-relevant covariances, if any, would undermine downstream assessments of multi-variate hazards (*e.g.,* droughts, flooding, and wildfires). Drought and wildfire metrics, for instance, may require self-consistent inputs of temperature and precipitation. Additionally, statistical downscaling assumes that observed functional relationships will be preserved in the future (*i.e.,* the stationarity assumption) despite climate change (Milly et al. 2008). A precise understanding of the extent to which such assumption may undermine projections nevertheless remains elusive.

Here we assess the extent to which locally relevant covariances between temperature and precipitation are preserved (or lost), as compared to outputs from global climate models and their dynamically downscaled counterparts, in two widely-used techniques for downscaling: LOCalized Analogs version 2 (LOCA2) and Seasonal Trends and Analysis of Residuals Empirical-Statistical Downscaling Model (STAR-ESDM). Specifically, we examine expected covariances between temperature and precipitation during convective and frontal precipitation events, including for the projection interval where the stationarity assumption may not hold. Although the credibility of both LOCA2 and STAR-ESDM has been evaluated for single variables (*e.g.,* Pierce et al., 2014; Hayhoe et al., 2023), we propose for the first time diagnostics

https://doi.org/10.5194/egusphere-2024-1456
Preprint. Discussion started: 5 June 2024

for evaluating *covariances* that can be applied universally to a wide range of statistically downscaled products. Collectively, our work attempts to address the following questions:

1) To what extent is physical consistency across variables preserved, as compared to observations, when variables are (i) statistically downscaled independently and (ii) dynamically downscaled concurrently?
2) How much does the stationarity assumption inherent in statistical downscaling undermine credibility of projections, particularly for potentially non-stationary hydrologic processes?

2. Data and Methods:

We employ outputs from eight Coupled Model Intercomparison Project Phase 6 (CMIP6) models and their statistically downscaled counterparts (see Table 1). The statistically downscaled products come from LOCalized Analogs version 2 (LOCA2; Pierce et al. 2014) and Seasonal Trends and Analysis of Residuals Empirical-Statistical Downscaling Model (STAR-ESDM). The following description of LOCA2 and STAR-ESDM is from Ullrich (2023), with minor modifications. LOCA2 is a statistical downscaling technique based on signal decomposition employing analogs (*i.e.,* days in the historical record that exhibit regional meteorology most like the regional patterns of a given day in the CMIP6 model). The LOCA2 algorithm first bias-corrects historical CMIP6 outputs to observations using quantile mapping. It then adjusts the amount of variability seen in different frequency bands to match observations using a digital filter (Pierce et al., 2014). To downscale data at a given grid cell, the 30 days in the historical record best exhibiting regional meteorology as compared to the CMIP6 model day is identified. The single day best matching the model day is used as the analog for the local region around the

https://doi.org/10.5194/egusphere-2024-1456
Preprint. Discussion started: 5 June 2024

grid point (Pierce et al., 2023). The LOCA2 North American product uses Livneh-unsplit data with 6-km grid spacing as the precipitation training data set and an updated version of Livneh et al. 2015 as the temperature training data set. Outputs from LOCA2 are available at 6-km grid resolution (Pierce et al, 2023).

STAR-ESDM is a statistical downscaling technique based on signal decomposition (Hayhoe et al., 2023). The STAR-ESDM algorithm first disaggregates observations and GCM outputs into four separate components: the long-term trend, the static climatology (mean annual cycle over historical), the dynamic climatology (mean annual cycle accounting for annual variations) and high-frequency (daily) anomalies. For each of these components, mappings are constructed between observations and historical GCM outputs. Future projections are bias-corrected using these mappings, then components are recombined to produce a consistent estimate of future time series. The STAR-ESDM product uses nClimGrid-Daily data with 5-km grid spacing for training over the contiguous United States (Durre et al., 2022).

We compare convective and frontal precipitation processes from (i) the European Centre for Medium-Range Weather Forecasts Reanalysis fifth Generation data (ERA5; Hersbach et al., 2020) against (ii) CMIP6 GCMs and their statically downscaled counterparts (LOCA2 and STAR-ESM). To ensure robustness of "ground truth," we also examine convective and frontal precipitation processes in the observation-based Livneh (Livneh et al. 2015) and nClimGrid-Daily (Durre et al., 2022) hydrometeorological datasets. Finally, to assess the extent to which the stationarity assumption affects projections across statistical and dynamical downscaling, we compare LOCA2 and STAR-ESMD against the North America component of the Coordinated Regional Downscaling Experiment (NA-CORDEX; Mearns et al. 2017). NA-CORDEX dynamically downscales climate model simulations under historical and Representative Concentration Pathway 8.5 W/m^2 (RCP8.5) forcings with a suite of regional climate models. We

https://doi.org/10.5194/egusphere-2024-1456
Preprint. Discussion started: 5 June 2024

employ five different raw GCM experiments downscaled with five different regional climate models (see Table 2) that provide daily outputs on ~ 25 km resolution.

Statistically downscaled products generally only provide a few variables at daily or higher frequencies, which can make it difficult to evaluate covariances. We therefore follow Zhang et al. (2023) in isolating for a single convective precipitation event each year by considering precipitation at each grid point coincident with the highest daily maximum temperature during that year (herein convective precipitation). Similarly, we isolate for a single (cold) frontal precipitation event each year by considering precipitation coincident with the greatest drop in surface temperature for that year (herein convective precipitation). For every grid point, our method thus identifies one convective precipitation event and one frontal precipitation event per year.

We examine daily near-surface temperature and precipitation fields during convective and frontal precipitation events over the contiguous US, focusing on a 21-day window from 10 days prior to and 10 days following the day of convective and frontal precipitation, respectively (and including the day of convective or frontal precipitation itself). Covariances between the two fields are calculated on a per-grid basis. For the raw GCMs and ERA5, we also examine moist static energy, which we estimate using daily temperature, specific humidity, and geopotential height, but substitute monthly surface pressure (due to data availability). Our comparisons provide a baseline for the performance of both the raw GCMs and the two statistical downscaling techniques. For the purposes of this study, we examine (i) a 35-year period spanning the 1980-2014 historical interval and (ii) a 35-year period spanning the 2065-2099 interval under the Shared Socioeconomic Pathway “Fossil Fueled Development” scenario with 8.5 W/m^2 of radiative forcing (SSP585). For dynamical downscaling outputs, we examine the 2065-2098 interval under the RCP8.5 forcing.

https://doi.org/10.5194/egusphere-2024-1456
Preprint. Discussion started: 5 June 2024

3. Results

3.1 Convective and frontal precipitation processes in observation-based datasets

We first examine convective and frontal precipitation in the ERA5 Reanalysis dataset (Figures 1, 2). Composite time series centered around the hottest day (day 0) shows surface temperature anomalies increase exponentially from -1K 10 days prior (day -10), peak at 3K on the hottest day (day 0), then decrease exponentially to -1K for the 10 days following (day + 10; Figure 1). Spatial composites of surface temperature on the hottest day show warm temperature anomalies broadly over the CONUS domain; spatial composites of the 10th day after show broad cool anomalies. Coincident precipitation time series show precipitation anomalies that decrease from day -10 to day 0 (co-occurring with temperature anomalies increasing). Precipitation anomalies are lowest on the hottest day (between -1 and -1.5 mm/day), with the spatial composite of day 0 showing broad dryness. Precipitation anomalies rapidly increase in the immediate days following coincidence with surface temperature anomaly decrease; the spatial composite of precipitation on day +10, for instance, shows broad wetting indicative of convective precipitation.

Our examination of surface temperature and precipitation are consistent with expectations of convective precipitation: surface temperature will rise until surface air convects, triggering precipitation and cooling surface air temperature. Analysis of coincident moist static energy reinforces this mechanism, as moist static energy increases until the precipitation event. Moist static energy moreover rapidly decreases immediately after the precipitation event as the atmosphere stabilizes. Parallel surface temperature and precipitation results for the observation-based Livneh (Supplemental Figure 1) and nClimGrid-Daily (Supplemental Figure 2) datasets

https://doi.org/10.5194/egusphere-2024-1456
Preprint. Discussion started: 5 June 2024

show similar results. Such consistency across ERA5 and the two observation-based products reinforce ERA5 to be reflective of "ground truth."

We next examine parallel time series and spatial composites for cold frontal precipitation, centered around the greatest drop in surface temperature (Figure 2). Composite time series show temperature anomalies to be highest on the day of frontal precipitation (day 0), drop to the lowest in the two days following (day +1 to +2), then return to ~zero by day +10. Spatial composites of surface temperature show warm anomalies over the CONUS domain on day 0 and cold anomalies on day +2. Coincident precipitation time series show precipitation anomalies that dramatically increase (from < 0 mm/day at day -2 to ~3.5 mm/day at day 0), before falling back to < 0 mm/day. Spatial composites of precipitation anomalies on the day of frontal precipitation show broad wetting, with the eastern half of the CONUS domain showing more significant anomalies. Spatial composites of precipitation anomalies at day +2 show largely neutral conditions over most of the CONUS domain. Analysis of moist static energy reinforces a cold frontal precipitation mechanism, with a steep decline in moist static energy that is coincident with a steep decline in surface temperature associated sudden precipitation.

To further evaluate our method of identifying precipitation events, we apply a discrete Fourier transform on days of the year when the convective and frontal precipitation events are occurring, respectively (Figure 3). We find that convective precipitation predominantly occurs in boreal summer (June-July-August; consistent with when warm days are prevalent). Frontal precipitation predominantly occurs in boreal winter (December-January-February; consistent with when cold fronts would be most prevalent), notwithstanding intermountain regions of the US West where orographic lifting is prevalent. Given the observed hydroclimatic co-variances and expected the seasonal occurrence, we conclude our methodology to be robust. We deem the physical relationships between surface temperature and precipitation observed in ERA5 during

https://doi.org/10.5194/egusphere-2024-1456
Preprint. Discussion started: 5 June 2024

convective and frontal precipitation (as identified in our methodology) to be appropriate for evaluate the credibility of GCMs and their statistically downscaled products.

3.2 Precipitation processes in raw and statistically downscaled GCMs over the historical interval

Some spread amongst the GCMs notwithstanding, the eight CMIP6 GCMs herein analyzed behave consistently with ERA5 for both convective and frontal precipitation over the 1980-2014 historical interval (Figure 4; see Table 1 for list of models). That is, convective precipitation anomalies consistently (i) decrease leading up to the hottest day; (ii) are lowest about the hottest day; then (iii) drastically increase with convection in the immediate days following. Frontal precipitation is moreover clearly visible in the GCMs, with drastic and acute precipitation evident centered around the day of greatest temperature decrease. The raw GCMs not only match the temporal evolution of surface temperature and precipitation as demonstrated in ERA5 but correctly simulate the magnitude of anomalies during convective and frontal precipitation events. Our results therefore indicate that the CMIP6 GCMs robustly capture convective and frontal precipitation processes.

We next examine these same co-variances after the GCMs are statically downscaled using LOCA2 and STAR-ESDM techniques (Figures 5, 6). For temperature, differences amongst the eight GCMs (*i.e.,* inter-model spread) are noticeably reduced post-downscaling for both convective and frontal precipitation (see surface temperature time series of the 21 days examined in Figures 5 and 6 and their respective standard deviations). This is somewhat expected, as the downscaling method bias-corrects the GCMs to "match" observations. Deviations in GCMs relative to observations (Livneh dataset for LOCA2 and nClimGrid-Daily dataset for STAR-

https://doi.org/10.5194/egusphere-2024-1456
Preprint. Discussion started: 5 June 2024

ESDM) will thus be minimized. Spatial composites of downscaled surface temperature, for instance, closely mirror those shown in ERA5 for both convective and frontal precipitation. In some cases, inter-model spread for precipitation can also be reduced, though this influence is less pronounced than for temperature. Note that bias-correction during statistical downscaling is performed variable by variable (*i.e.,* independently and without explicit consideration of local co-variances across variables) and that our definitions of convective and frontal precipitation in effect selects precipitation fields based on surface temperature characteristics. Inter-model spread for downscaled precipitation fields are thus not explicitly expected to get smaller. Our results nevertheless suggest that the LOCA2 and STAR-ESDM downscaling techniques generally preserve or limit inter-model spread in co-variances shown in the raw GCMs with high fidelity (compare, for instance, mean absolute error values for raw GCMs against their downscaled counterparts in Figures 4-6).

There are nevertheless clear ensemble-mean differences between the downscaled products and the raw GCMs (and by extension ERA5 which the raw GCMs simulate with high skill) that require careful attention. LOCA2 appears nearly identical to ERA5 for convective precipitation. For frontal precipitation, however, the downscaling clearly dampens frontal precipitation relative to ERA5 and the raw GCMs by up to ~2 mm/day (Figures 4, 5): LOCA2 frontal precipitation (i) peaks at lower anomaly values (2.5 mm/day for the ensemble mean) than in ERA5 (3.9 mm/day) in the composite time series and (ii) the wet pattern apparent in the ERA5 composite is diminished in ensemble mean spatial composite. Importantly, such dampening is robust across most of the LOCA2 ensemble (Figure 5), indicating it to be an emergent feature of the LOCA2 downscaling method. STAR-ESDM does not exhibit this dampening: it shows frontal precipitation anomalies that closely match the frontal precipitation anomalies of ERA5 and the raw GCMs (Figure 6j-l). However, STAR-ESDM may slightly overshoot drying

https://doi.org/10.5194/egusphere-2024-1456
Preprint. Discussion started: 5 June 2024

anomalies prior to convective precipitation (by less than ~0.5 K). This influence is nevertheless modest and the STAR-ESDM ensemble simulates a range that encapsulates the evolution of frontal precipitation shown in ERA5.

3.3 Precipitation processes in raw and statistically downscaled GCMs over the future interval

We next examine convective and frontal precipitation in the raw GCMs over the future interval (2065-2099; Figure 7). For convective precipitation, the co-evolution of surface temperature and precipitation (including the magnitude of their respective anomalies) does not change substantially across the ensemble mean relative to the historical interval (compare Figure 4a-c to Figure 7a-c). For frontal precipitation, however, there is robust intensification that is present across all ensemble members: frontal precipitation peaks at ~ 4 mm/day over the historical interval (Figure 4e) but ~5-6 mm/day in the future interval (Figure 7e). Scatterplots of surface temperature and peak frontal precipitation (Supplemental Figure 3) show steeper associations between the two in the future interval, indicating that frontal precipitation to be driven at least in part by temperature increases. Moist static energy levels prior to frontal precipitation are also greater in the future interval, across the whole ensemble, relative to the historical interval (compare Figure 4f to Figure 7f), consistent with frontal precipitation intensification.

We again examine these same co-variances after the GCMs are statically downscaled for the future interval. Future interval time series and spatial composite results for both LOCA2 and STAR-ESDM products appear nearly identical to those of the historical interval, respectively, for convective precipitation (Figures 8a-f, 9a-f). This is consistent with expectations, as the raw GCMs themselves do not show appreciable changes for convective precipitation relative to the

https://doi.org/10.5194/egusphere-2024-1456
Preprint. Discussion started: 5 June 2024

historical interval. Robust intensification of frontal precipitation relative to the historical interval (that is otherwise robustly simulated by the raw GCMs) is not evident in LOCA2 (Figure 8g-i), some slight wetting notwithstanding. The LOCA2 method dampens frontal precipitation over both the historical and future intervals; the net effect is that it substantially underestimates future frontal precipitation relative to the raw GCMs. For instance, frontal precipitation anomalies reach ~7 mm/day in the raw GCMs but less than 4 mm/day in LOCA2 (and as low as a little as 2 mm/day). Frontal precipitation is intensified in STAR-ESDM (Figure 9j-l; ~4-6 mm/day in the future interval compared to ~3-5 mm/day in the historical interval), although the magnitude of the intensification falls short of what is simulated by the raw GCMs.

3.4 Precipitation processes post dynamically downscaling

Finally, we examine how convective and frontal precipitation processes are affected post *dynamical* downscaling across five different regional climate models. Dynamical downscaling of ERA5 preserves expected hydroclimate covariances during convective and frontal precipitation processes, some inter-regional model differences notwithstanding (Supplemental Figure 4; note that such differences are entirely attributable to regional climate models as the underlying data being downscaled is identical across the five models). Biases in regional climate models appear to be relatively small and are not prohibitive in representing convective and frontal precipitation processes on local-scales. These biases are also small when GCM data, instead of observation data, is downscaled. Convective precipitation processes post dynamical downscaling of GCMs in the future interval do not change much relative to the historical interval, consistent with the raw GCMs and with statistical downscaling (Supplemental Figure 4). However, we find that dynamical downscaling preserves robust intensification of future frontal precipitation simulated

https://doi.org/10.5194/egusphere-2024-1456
Preprint. Discussion started: 5 June 2024

by raw GCMs, in strong contrast to the dampening of this intensification seen with statistical downscaling. The finding is robust across all five regional climate models examined, indicating low sensitivity to regional model biases. Frontal precipitation in the future interval post dynamical downscaling is ~1.5 mm/day to 2 mm/day greater than in the historical interval, which is very much consistent with the magnitude of intensification seen with the raw GCMs.

4. Conclusions

We have employed expected covariances between surface temperature and precipitation during convective and frontal precipitation events as diagnostics to evaluate the credibility of two statistical downscaling techniques. We find that statistical downscaling generally preserves covariances during convective precipitation over both the historical and future intervals. Statistical downscaling also preserves expected covariances during frontal precipitation events over the historical interval; however, the downscaling dampens projected intensification of frontal precipitation in the future interval that is otherwise robustly simulated in the raw CMIP6 GCMs (*i.e.,* prior to downscaling) and with dynamical downscaling. We conclude the dampening to be a spurious feature of the LOCA2 and STAR-ESDM downscaling technique, presumably from historical functional relationships and/or the non-stationarity assumption therein.

Note that convective precipitation as examined in our analyses do not exhibit material differences across the historical and future intervals (as opposed to frontal precipitation which show robust intensification in the future interval). Convective precipitation is therefore likely insensitive to the stationarity assumption, notwithstanding the possibility that CMIP6 models themselves may not effectively resolve global cloud-systems (and thus may not capture non-stationary changes in convective precipitation). More broadly, our frontal precipitation results

https://doi.org/10.5194/egusphere-2024-1456
Preprint. Discussion started: 5 June 2024

suggest that statistical downscaling may not capture structural changes to meteorological phenomena under non-stationarity. This is in strong contrast to dynamical downscaling (regardless of the regional climate model chosen), which preserves non-stationary physical relationships among variables and is thus able to capture such changes to meteorological phenomena. Such considerations may serve as limitations to the credibility of downscaled projections, particularly when considering the dominant (*e.g.,* Baek et al. 2019, 2021) and/or non-stationary (*e.g.,* Baek et al. 2020; Scholz et al. 2022) nature of internal atmospheric variability in driving hydrologic hazards. Importantly, our work highlights expected covariances during convective and frontal precipitation as process-based evaluation diagnostics that can be applied universally to a wide range of statistically downscaled products.

https://doi.org/10.5194/egusphere-2024-1456
Preprint. Discussion started: 5 June 2024

Figures

CMIP6 Models Analyzed	
CanESM5	INM-CM5-0
TaiESM1*	NorESM2-MM
FGOALS-g3	GFDL-ESM4
EC-Earth3	BCC-CSM2-MR

Table 1: List of CMIP6 models analyzed. All models use the r1i1p1f1 member. We examine the same eight models in the LOCA2 and STAR-ESDM downscaled data. *TaiESM1 is only analyzed over the historical interval (and not the future interval) for the raw GCM due to data availability.

https://doi.org/10.5194/egusphere-2024-1456
Preprint. Discussion started: 5 June 2024

	RegCM4	WRF	CRCM5-OUR	CRCM5-UQAM	CanRCM4
ERA-Int	Analyzed	Analyzed	Analyzed	Analyzed	Analyzed
HadGEM2-ES	Analyzed				
CanESM2					Analyzed
MPI-ESM-MR				Analyzed	
CNRM-CM5			Analyzed		
GFDL-ESM2M		Analyzed			

335 **Table 2:** Simulation matrix adapted from NA-CORDEX. Left column shows the underlying data being dynamically downscaled. Top row shows the regional climate model driving the downscaling. The simulations analyzed are marked by "Analyzed" in the matrix.

https://doi.org/10.5194/egusphere-2024-1456
Preprint. Discussion started: 5 June 2024

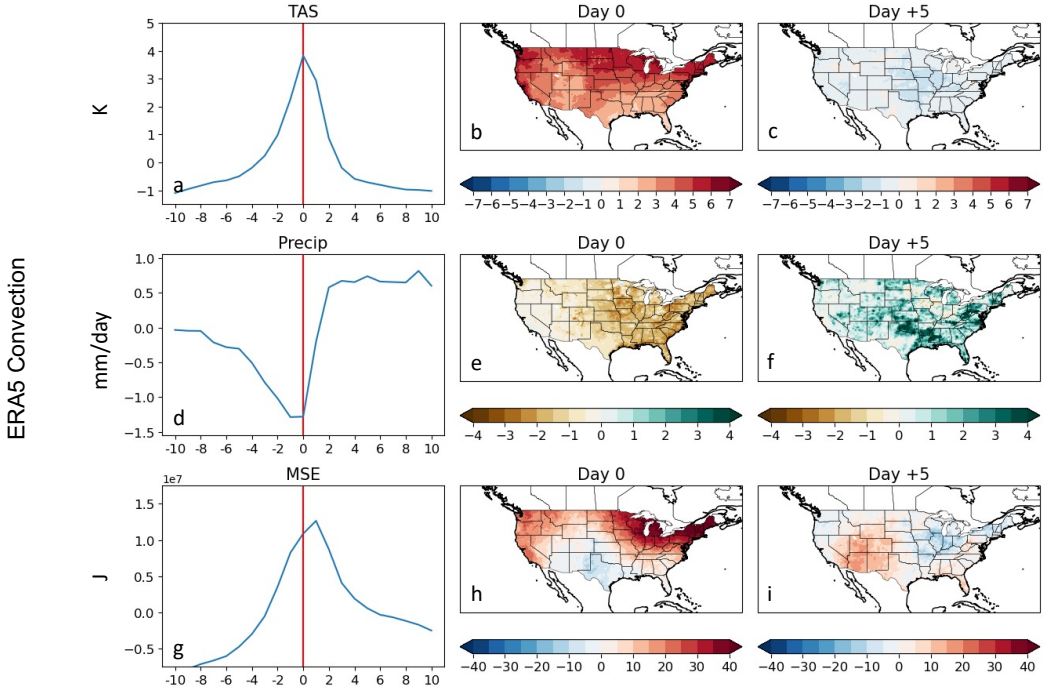

Figure 1: (a) 21-day composite time series of CONUS surface temperature anomalies centered around the day of convective precipitation using ERA5 data over the 1980-2014 interval. **(b)** Spatial composite of surface temperature on the day of convective precipitation **(c)** Spatial composite 5 days after convective precipitation **(d-f)** Same as (a-c) but for precipitation. (**g-i)** Same as (a-c) but for moist static energy (MSE).

https://doi.org/10.5194/egusphere-2024-1456
Preprint. Discussion started: 5 June 2024

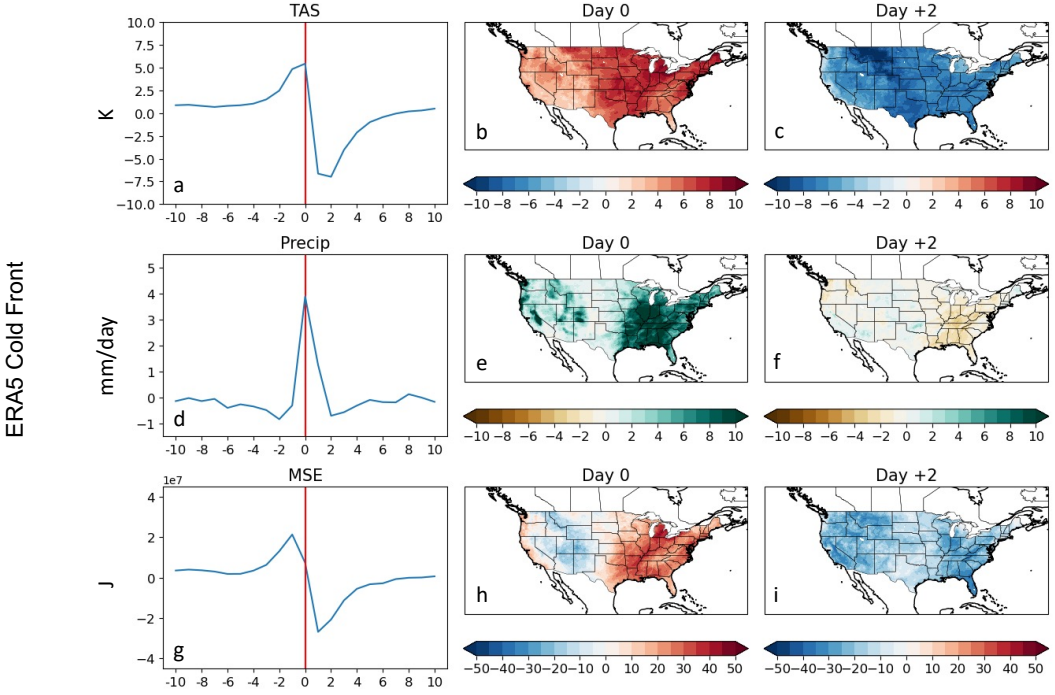

Figure 2: (a) 21-day composite time series of CONUS surface temperature centered around the day of cold frontal precipitation using ERA5 data over the 1980-2014 interval. **(b)** Spatial composite of surface temperature anomalies on the day of convective precipitation **(c)** Spatial composite of surface temperature anomalies two days following the day of frontal precipitation **(d-f)** Same as (a-c) but for precipitation. (**g-i)** Same as (a-c) but for moist static energy.

https://doi.org/10.5194/egusphere-2024-1456
Preprint. Discussion started: 5 June 2024

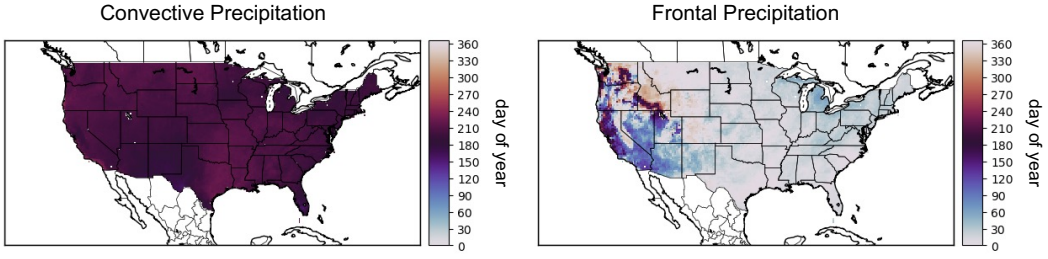

Figure 3: Peak convective and frontal day of year. Peak day is determined using a discrete Fourier transform.

https://doi.org/10.5194/egusphere-2024-1456
Preprint. Discussion started: 5 June 2024

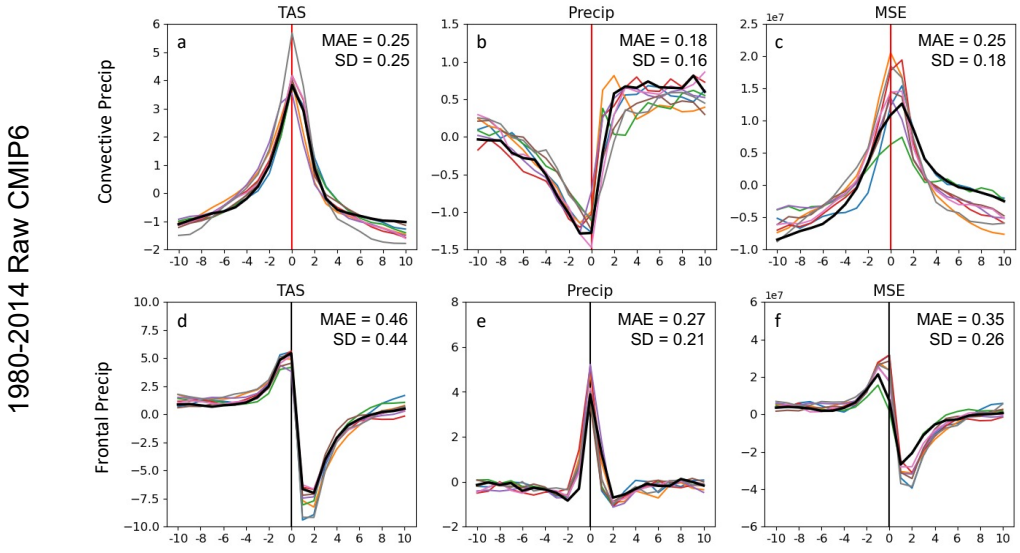

Figure 4: 21-day composite time series of **(a)** surface temperature (K), **(b)** precipitation (mm/day), and **(c)** moist static energy (10^7 Joules) over CONUS for (colored lines; list of GCMs provided in Table 1) raw CMIP6 GCM and (solid black line) ERA5 data. Time series are centered around the day of convective precipitation and for the 1980-2014 period **(d-f)** Same as (a-c) but for frontal precipitation.

https://doi.org/10.5194/egusphere-2024-1456
Preprint. Discussion started: 5 June 2024

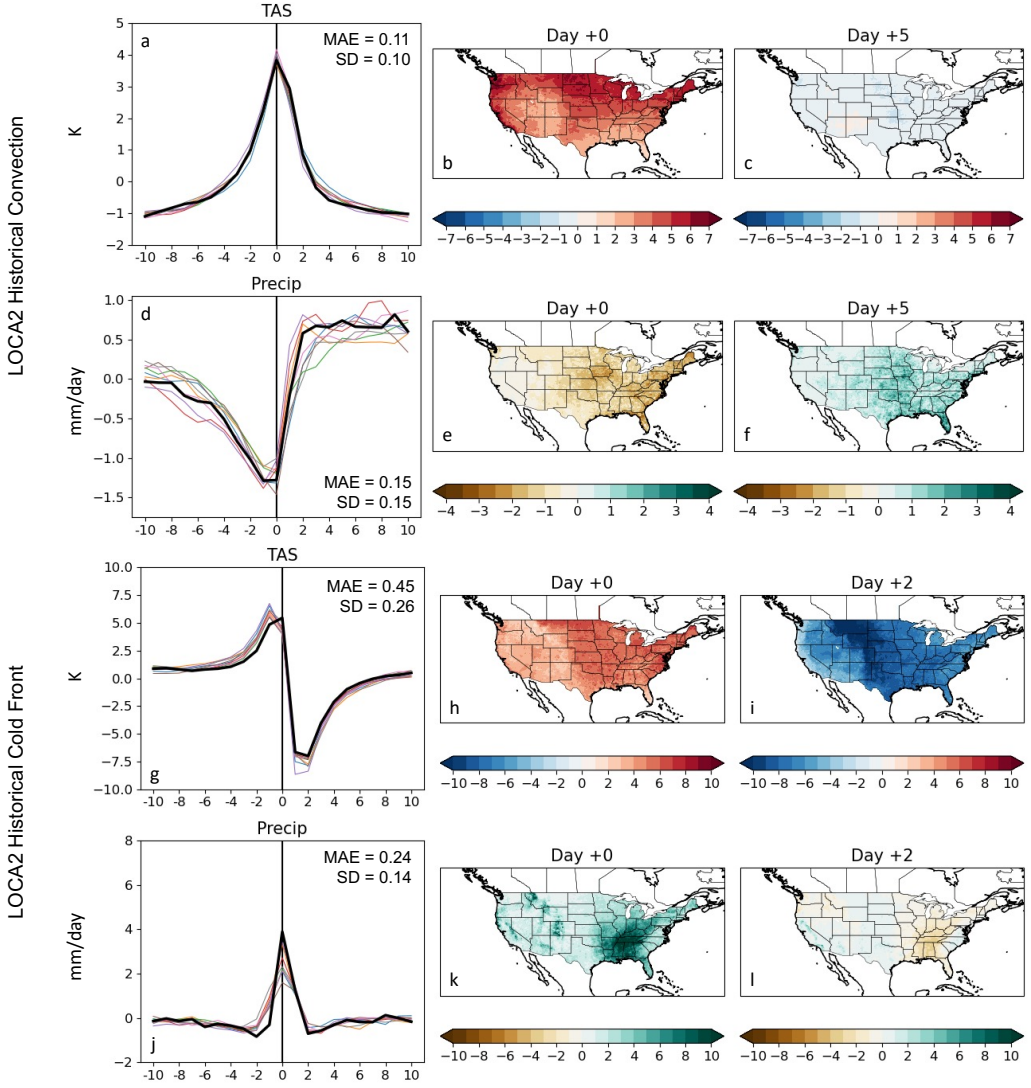

Figure 5: (a) 21-day composite time series of CONUS surface temperature centered around the day of convective precipitation using (colored lines) LOCA2 data over the 1980-2014 interval. Solid black line shows ERA5 data. **(b)** Spatial composite of surface temperature on the day of convective precipitation using LOCA2. **(c)** Spatial composite of surface temperature 10 days prior to convective precipitation using LOCA2 **(d-f)** Same as (a-c) but for precipitation. **(g)** 21-day composite time series of CONUS surface temperature centered around the day of frontal precipitation using (colored lines) LOCA2 data over the 1980-2014 interval. Solid black line shows ERA5 data. **(h)** Spatial composite of surface temperature on the day of convective precipitation using LOCA2 data. **(i)** Spatial composite of surface temperature 10 days prior to convective precipitation using LOCA2 data **(j-l)** Same as (g-i) but for precipitation. Mean absolute error (MAE) is calculated between (i) ERA5 time series and (ii) LOCA2 time series and provided in lower right corner of (a, d, g, j).

https://doi.org/10.5194/egusphere-2024-1456
Preprint. Discussion started: 5 June 2024

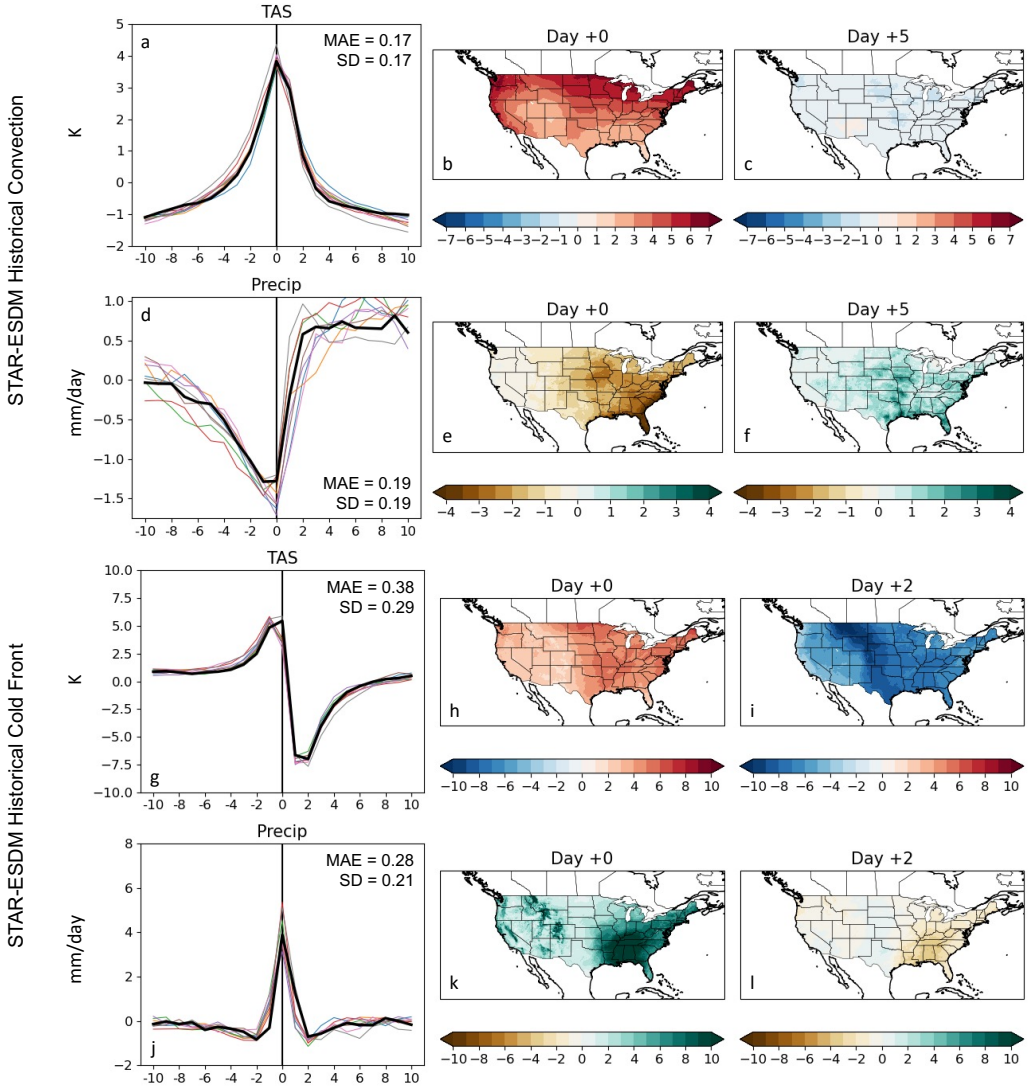

380 **Figure 6:** Same as Figure 5, but for STAR-ESDM data.

https://doi.org/10.5194/egusphere-2024-1456
Preprint. Discussion started: 5 June 2024

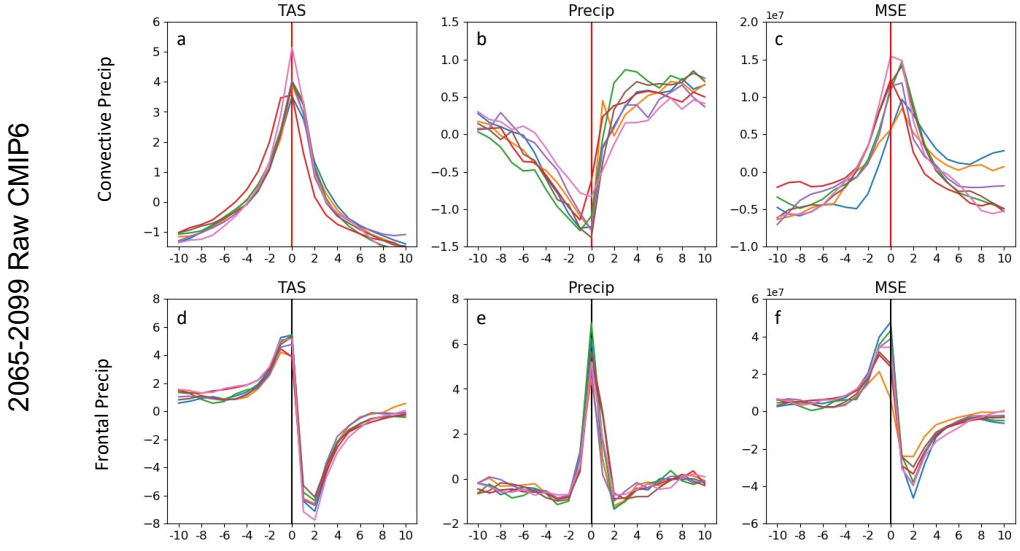

385 **Figure 7:** Same as Figure 4, but for the 2065-2099 interval under SSP585 forcing.

https://doi.org/10.5194/egusphere-2024-1456
Preprint. Discussion started: 5 June 2024

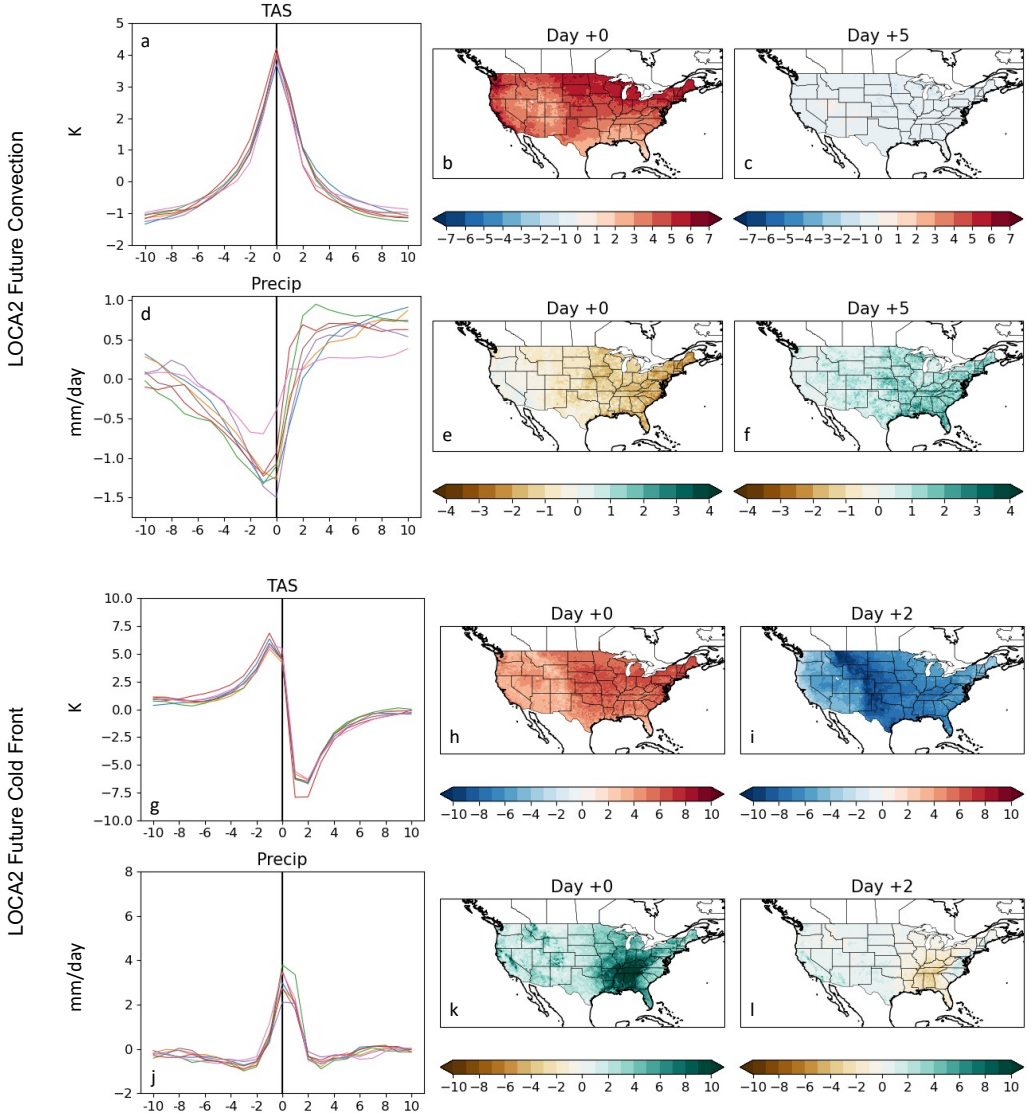

Figure 8: Same as Figure 5, but for the 2065-2099 interval under SSP585 forcing.

https://doi.org/10.5194/egusphere-2024-1456
Preprint. Discussion started: 5 June 2024

390

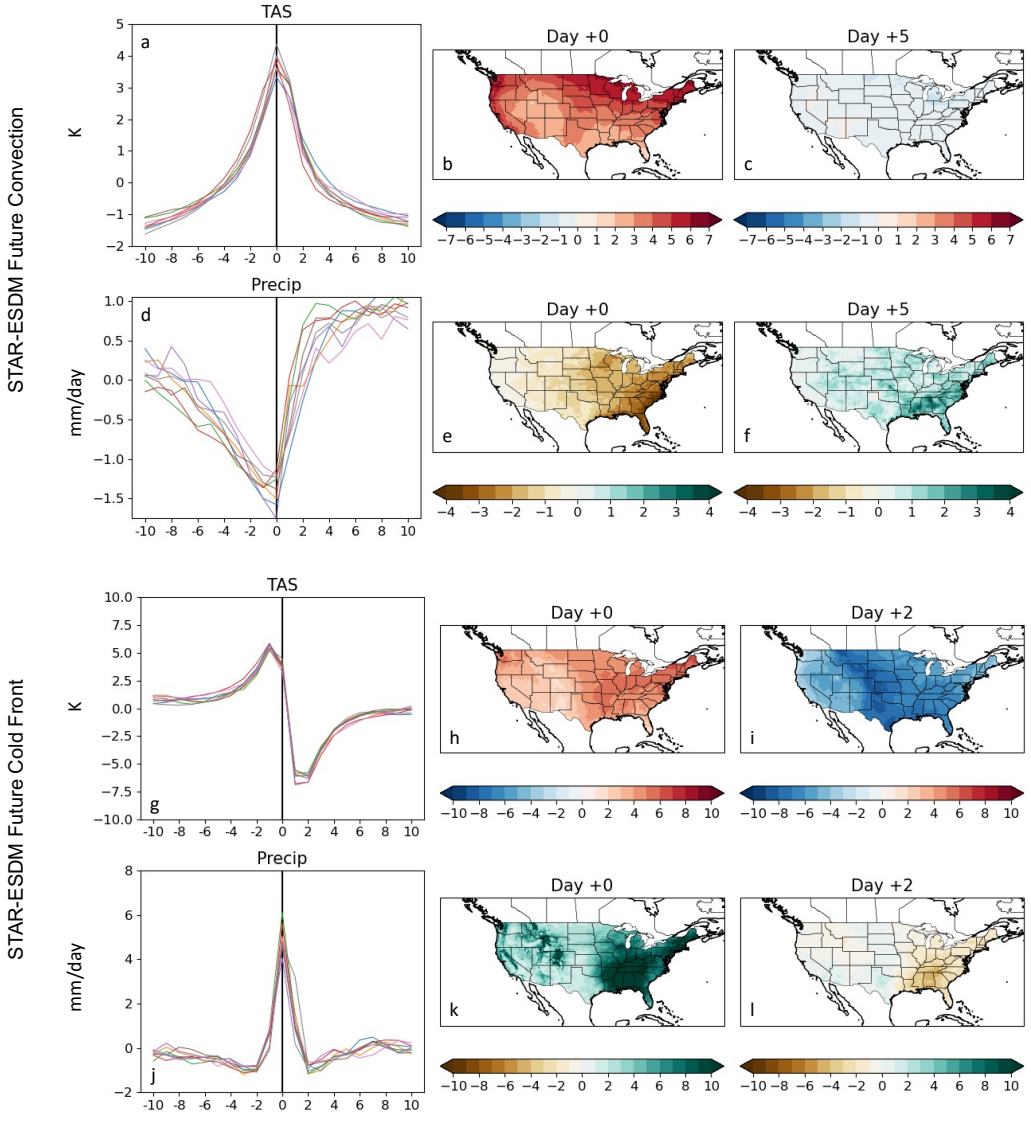

Figure 9: Same as Figure 6, but for STAR-ESDM data.

https://doi.org/10.5194/egusphere-2024-1456
Preprint. Discussion started: 5 June 2024

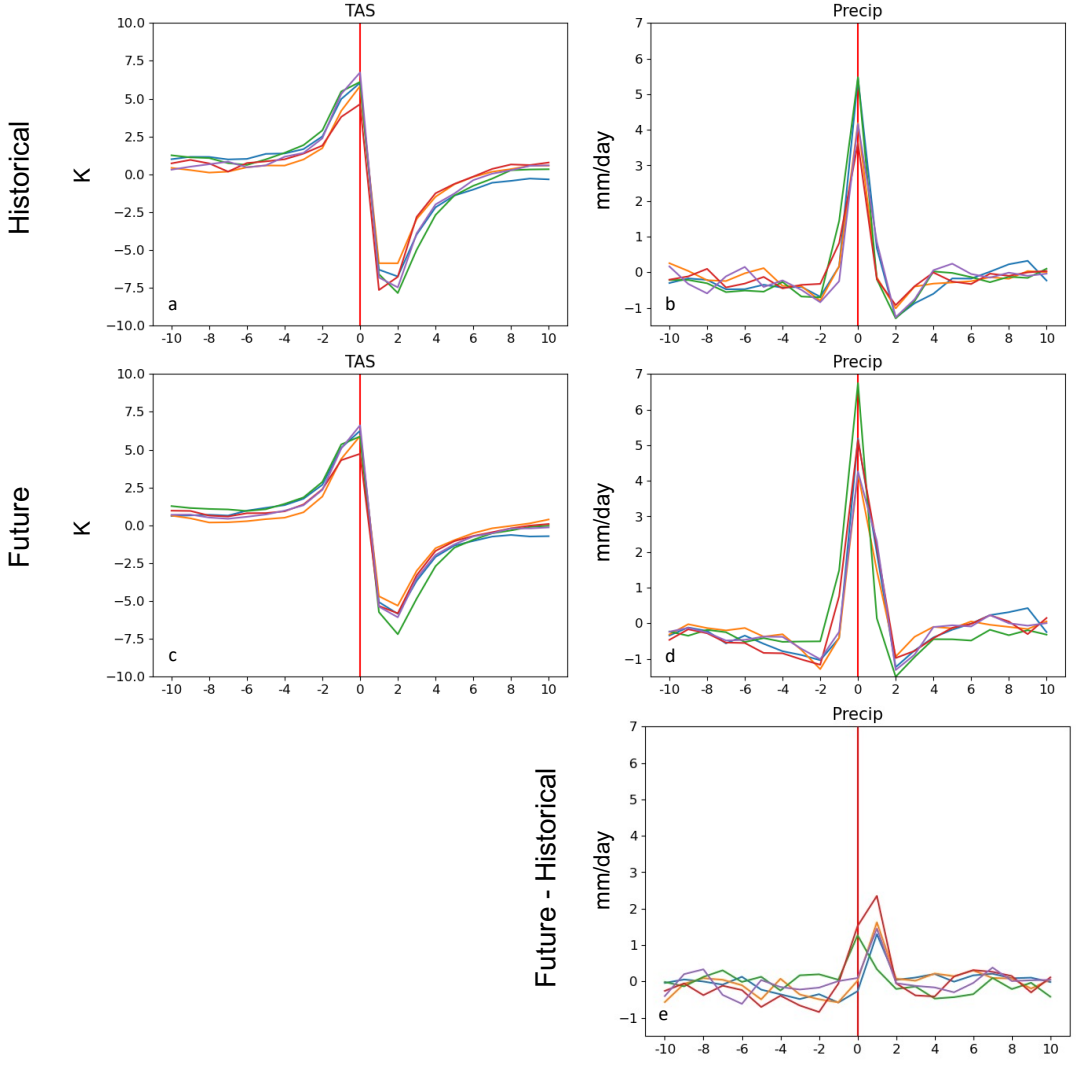

Figure 10: 21-day composite time series of CONUS **(a)** surface temperature and **(b)** precipitation anomalies centered around the day of convective precipitation using dynamical downscaling of GCM data over the 1980-2014 interval. (**c-d)** Same as (a-b) but for the future interval over 2065-2098 under RCP8.5 forcing. **(e)** Difference between (d) and (b).

https://doi.org/10.5194/egusphere-2024-1456
Preprint. Discussion started: 5 June 2024

Code and Data Availability

Code required to conduct the analyses herein are available on https://zenodo.org/records/11194306. All data used in this study are publicly available. The raw CMIP6 GCM data can be downloaded from the USA portal of the Earth System Grid Federation (https://aims2.llnl.gov/search/cmip6/). ERA5 data can be downloaded from the Copernicus Climate Data Store (https://cds.climate.copernicus.eu/cdsapp#!/dataset/reanalysis-era5-single-levels?tab=form). NA-CORDEX data can be downloaded from the National Center for Atmospheric Research Climate Data Gateway (https://www.earthsystemgrid.org/search/cordexsearch.html). Livneh data can be downloaded from the National Centers for Environmental Information at (https://www.ncei.noaa.gov/access/metadata/landing-page/bin/iso?id=gov.noaa.nodc:0129374). The nClimGrid-Daily data can also be downloaded from the National Centers for Environmental Information at (https://www.ncei.noaa.gov/products/land-based-station/nclimgrid-daily). LOCA2 data can be downloaded from (https://cirrus.ucsd.edu/~pierce/LOCA2/). The STAR-ESDM data can be downloaded from (https://app.globus.org/file-manager?origin_id=9d6d994a-6d04-11e5-ba46-22000b92c6ec&origin_path=%2Fglobal%2Fcfs%2Fprojectdirs%2Fm3522%2Fcmip6%2FSTAR-ESDM%2Fssp585%2F&two_pane=true).

Author contributions

S.H.B. and P.A.U. designed the study. S.H.B. performed the analyses and wrote the paper, with contributions from all co-authors.

Competing interests

The authors declare no competing interests.

Acknowledgements

This work was performed under the auspices of the U.S. Department of Energy by Lawrence Livermore National Laboratory under contract DE-AC52-07NA27344. The authors would like to acknowledge the Lab Directed Research and Development program 50385-23ERD050. LLNL-JRNL863969.

https://doi.org/10.5194/egusphere-2024-1456
Preprint. Discussion started: 5 June 2024

References

Abatzoglou, J.T. and T.J. Brown (2012) "A comparison of statistical downscaling methods suited for wildfire applications." *Int. J. Climatol.*, *32*(5), 772-780, doi: 10.1002/joc.2312.

Arnell, N. W., Lowe, J. A., Bernie, D., Nicholls, R. J., Brown, S., Challinor, A. J., & Osborn, T. J. (2019). The global and regional impacts of climate change under representative concentration pathway forcings and shared socioeconomic pathway socioeconomic scenarios. *Environmental Research Letters*, 14(8), 084046. https://doi.org/10.1088/1748-9326/ab35a6

Baek, S. H., Smerdon, J. E., Seager, R., Williams, A. P., & Cook, B. I. (2019). Pacific Ocean forcing and atmospheric variability are the dominant causes of spatially widespread droughts in the contiguous United States. *Journal of Geophysical Research: Atmospheres*, 124, 2507–2524. https://doi.org/10.1029/2018JD029219

Baek, S.H., Smerdon, J.E., Dobrin, GC. *et al.* A quantitative hydroclimatic context for the European Great Famine of 1315–1317. *Commun Earth Environ* **1**, 19 (2020). https://doi.org/10.1038/s43247-020-00016-3

Baek, S. H., J. E. Smerdon, B. I. Cook, and A. P. Williams, 2021: U.S. Pacific Coastal Droughts Are Predominantly Driven by Internal Atmospheric Variability. *J. Climate*, **34**, 1947–1962, https://doi.org/10.1175/JCLI-D-20-0365.1.

Bourgault et al., (2023). xclim: xarray-based climate data analytics. Journal of Open Source Software, 8(85), 5415, https://doi.org/10.21105/joss.05415

Cash, D., W.C. Clark, F. Alcock, N.M. Dickson, N. Eckley and J. Jäger (2002) Salience, credibility, legitimacy and boundaries: linking research, assessment and decision making. *Assessment and Decision Making (November 2002)*, doi: 10.2139/ssrn.372280.

Chen, X., L.R. Leung, Y. Gao, Y. Liu and M. Wigmosta (2023) Sharpening of cold-season storms over the western United States. *Nature Climate Change*, doi: 10.1038/s41558-022-01578-0.

Dai, A., Rasmussen, R.M., Ikeda, K. *et al.* A new approach to construct representative future forcing data for dynamic downscaling. *Clim Dyn* **55**, 315–323 (2020). https://doi.org/10.1007/s00382-017-3708-8

Durre, I., M. F. Squires, R. S. Vose, A. Arguez, W. S. Gross, J. R. Rennie, and C. J. Schreck, 2022: NOAA's nClimGrid-Daily Version 1 – Daily gridded temperature and precipitation for the Contiguous United States since 1951. NOAA National Centers for Environmental Information, since 6 May 2022, https://doi.org/10.25921/c4gt-r169

Eyring, V., Bony, S., Meehl, G. A., Senior, C. A., Stevens, B., Stouffer, R. J., and Taylor, K. E.: Overview of the Coupled Model Intercomparison Project Phase 6 (CMIP6) experimental design

https://doi.org/10.5194/egusphere-2024-1456
Preprint. Discussion started: 5 June 2024

and organization, Geosci. Model Dev., 9, 1937–1958, https://doi.org/10.5194/gmd-9-1937-2016, 2016.

Fiedler, T., Pitman, A.J., Mackenzie, K. *et al.* Business risk and the emergence of climate analytics. *Nat. Clim. Chang.* **11**, 87–94 (2021). https://doi.org/10.1038/s41558-020-00984-6

Hayhoe, K., Stoner, A., Wuebbles, D. J. et al. (2023) STAR-ESDM: A Generalizable Approach to Generating High-Resolution Climate Projections through Signal Decomposition. *ESS Open Archive*. **DOI: 10.22541/essoar.169462036.65393270/v1**

Hersbach H, Bell B, Berrisford P, et al. The ERA5 global reanalysis. *Q J R Meteorol Soc*. 2020; 146: 1999–2049. https://doi.org/10.1002/qj.3803Hofmann, M., Volosciuk, C., Dubrovský, M., Maraun, D., and Schultz, H. R.: Downscaling of climate change scenarios for a high-resolution, site-specific assessment of drought stress risk for two viticultural regions with heterogeneous landscapes, Earth Syst. Dynam., 13, 911–934, https://doi.org/10.5194/esd-13-911-2022, 2022.

Jones, A.D., Rastogi, D., Vahmani, P. *et al.* Continental United States climate projections based on thermodynamic modification of historical weather. *Sci Data* **10**, 664 (2023). https://doi.org/10.1038/s41597-023-02485-5

Keetch, John J; Byram, George. 1968. A drought index for forest fire control. Res. Paper SE-38. Asheville, NC: U.S. Department of Agriculture, Forest Service, Southeastern Forest Experiment Station. 32 pp. (Revised 1988).

Lee, JW., Hong, SY. Potential for added value to downscaled climate extremes over Korea by increased resolution of a regional climate model. *Theor Appl Climatol* **117**, 667–677 (2014). https://doi.org/10.1007/s00704-013-1034-6

Liu, C., K. Ikeda, R. Rasmussen, M. Barlage, A.J. Newman, A.F. Prein, F. Chen, L. Chen, M. Clark, A. Dai and J. Dudhia (2017). Continental-scale convection-permitting modeling of the current and future climate of North America. Climate Dynamics, 49(1), 71-95, doi: 10.1007/s00382-016-3327-9.

Livneh, B., T. J. Bohn, D. W. Pierce, F. Munoz-Arriola, B. Nijssen, R. Vose, D. R. Cayan, and L. Brekke, 2015: A spatially comprehensive, hydrometeorological data set for Mexico, the U.S., and Southern Canada 1950–2013. *Scientific Data*, 2, https://doi.org/10.1038/sdata.2015.42.

Mearns, L.O., et al., 2017: *The NA-CORDEX dataset*, version 1.0. NCAR Climate Data Gateway, Boulder CO, accessed [date], https://doi.org/10.5065/D6SJ1JCH

Milly PC, Betancourt J, Falkenmark M, Hirsch RM, Kundzewicz ZW, Lettenmaier DP, Stouffer RJ (2008). Climate change. Stationarity is dead: whither water management? Science. 319(5863):573-4. doi: 10.1126/science.1151915.

NOAA National Centers for Environmental Information (NCEI) U.S. Billion-Dollar Weather and Climate Disasters (2023). https://www.ncei.noaa.gov/access/billions/, DOI: 10.25921/stkw-7w73

https://doi.org/10.5194/egusphere-2024-1456
Preprint. Discussion started: 5 June 2024

Pierce, D. W., D.R. Cayan, and B.L. Thrasher (2014) Statistical downscaling using Localized Constructed Analogs (LOCA). *J. Hydrometeor.*, 15, 2558-2585, doi: JHM-D-14-0082.1.

Pierce, D. W., Cayan, D. R., Feldman, D. R., & Risser, M. D. (2023). Future Increases in North American Extreme Precipitation in CMIP6 Downscaled with LOCA. Journal of Hydrometeorology, 24(5), 951-975. https://doi.org/10.1175/JHM-D-22-0194.1

Pitman, A. J., Fiedler, T., Ranger, N., Jakob, C., Ridder, N., Perkins-Kirkpatrick, S. E., Wood, N., & Abramowitz, G. (2022). Acute climate risks in the financial system: examining the utility of climate model projections. Environmental Research, 1(2), 025002. https://doi.org/10.1088/2752-5295/ac856f

Rahimi, S. (2022). Memo on the Development and Availability of Dynamically Downscaled Projections Using WRF. California Energy Commission, https://www.energy.ca.gov/sites/default/files/2022-09/20220907_CDAWG_MemoDynamicalDownscaling_EPC-20-006_May2022-ADA.pdf

Rasmussen, R. et al. (2023) "CONUS404: The NCAR-USGS 4-km long-term regional hydroclimate reanalysis over the CONUS." *Bull. of Amer. Meteo. Soc.*, Submitted, doi: 10.1007/s00382-016-3327-9.

Scholz, S.R., Seager, R., Ting, M. et al. Changing hydroclimate dynamics and the 19th to 20th century wetting trend in the English Channel region of northwest Europe. *Clim Dyn* 58, 1539–1553 (2022). https://doi.org/10.1007/s00382-021-05977-5

TCFD, Recommendations of the Task Force on Climate-related Financial Disclosures, Task Force on Climate-related Financial Disclosures, Financial Stability Board, Basel, Switzerland, 2017

Thrasher, B., Maurer, E. P., McKellar, C., and Duffy, P. B. (2012). Technical Note: Bias correcting climate model simulated daily temperature extremes with quantile mapping, Hydrol. Earth Syst. Sci., 16, 3309–3314, https://doi.org/10.5194/hess-16-3309-2012.

Thrasher, B., Wang, W., Michaelis, A. et al. NASA Global Daily Downscaled Projections, CMIP6. Sci Data 9, 262 (2022). https://doi.org/10.1038/s41597-022-01393-4

Ullrich, P. A. (2023). Validation of LOCA2 and STAR-ESDM statistically downscaled products. https://doi.org/10.2172/2202926

Xu, Z., Han, Y. & Yang, Z. Dynamical downscaling of regional climate: A review of methods and limitations. Sci. China Earth Sci. 62, 365–375 (2019). https://doi.org/10.1007/s11430-018-9261-5

Zhang, Y., & Boos, W. R. (2023). An upper bound for extreme temperatures over midlatitude land. *Proceedings of the National Academy of Sciences of the United States of America*, *120*(12). https://doi.org/10.1073/pnas.2215278120